HHS Public Access

Author manuscript

Int J Cardiol. Author manuscript; available in PMC 2019 May 15.

Published in final edited form as:

Int J Cardiol. 2018 May 15; 259: 153–162. doi:10.1016/j.ijcard.2018.01.036.

AMP-activated protein kinase protects against necroptosis via regulation of Keap1-PGAM5 complex

Yi-Shu Wang[a,#,1], **Peng Yu**[b,#,1], **Yong Wang**[c,#,1], **Jing Zhang**[d,1], **Wei Hang**[c,e,1], **Zhi-Xian Yin**[e,1], **Gang Liu**[e,1], **Jianfeng Chen**[c,1], **Kaitlin D. Werle**[c,1], **Cheng-Shi Quan**[a,1], **Hang Gao**[a,1], **Qinghua Zeng**[a,1], **Rutao Cui**[f,1], **Jiyong Liang**[g,1], **Qiang Ding**[h,1], **Yu-Lin Li**[a,1,*], and **Zhi-Xiang Xu**[a,c,*,1]

[a]Key Laboratory of Pathobiology, Ministry of Education, Norman Bethune College of Medicine, Jilin University, Changchun, China

[b]Department of Endocrinology and Metabolism, The Second Affiliated Hospital of Nanchang University, Nanchang, Jiangxi, China

[c]Division of Hematology and Oncology, Comprehensive Cancer Center, University of Alabama at Birmingham, Birmingham, Alabama, USA

[d]Department of Anesthesiology, The Second Affiliated Hospital of Nanchang University, Nanchang, Jiangxi, China

[e]Department of Otorhinolaryngology Head and Neck Surgery, Tianjin Huanhu Hospital, Tianjin, China

[f]Department of Dermatology, Boston University, School of Medicine, Boston, Massachusetts, USA

[g]Department of Systems Biology, UT MD Anderson Cancer Center, Texas, USA

[h]Division of Pulmonary, Allergy, and Critical Care Medicine, Department of Medicine, University of Alabama Birmingham, Birmingham, AL, USA

Abstract

Background—The AMP-activated protein kinase (AMPK) plays critical roles in growth regulation and metabolism reprogramming. AMPK activation protects cells against apoptosis from injury in different cell and animal models. However, its function in necroptosis remains largely unclear.

[*]Corresponding authors: Zhi-Xiang Xu, M.D., Ph.D., zhixiangxu08@gmail.com or Yu-Lin Li, M.D., Ph.D., ylli@jlu.edu.cn, Key Laboratory of Pathobiology, Ministry of Education, Norman Bethune College of Medicine, Jilin University, 126 Xin-Min Ave., Changchun, Jilin, China. Tel: 011-86-431-85619481; Fax: 011-86-431-85619470.

[#]Y.S.W., P.Y. and Y.W. contributed equally.

[1]This author takes responsibility for all aspects of the reliability and freedom from bias of the data presented and their discussed interpretation.

Conflicts of Interest: The authors declare no conflict of interest.

Funding sources

This work was partially supported by the National Natural Science Foundation of China (Nos. 81573087 and 81772924 to Z.X.X., No. 81572139 to Y.L.L., No. 81760050 to P.Y., and No. 81760048. to J.Z.) and by the U.S. National Institutes of Health (R01CA133053 to Z.X.X.).

Methods and Results—In the current study, we demonstrated that AMPK was activated upon necroptosis induction and protected mouse embryonic fibroblasts (MEFs) and cardiomyocytes from N-methyl-N′-nitro-N-nitrosoguanidine (MNNG) and reactive oxygen species (ROS) induced necroptosis. Activation of AMPK with chemicals A-769662, 2-deoxyglucose (2-DG), and metformin or constitutively active (CA) AMPK markedly decreased necroptosis and cytotoxicity induced by MNNG. In contrast, AMPK inhibitor compound C, dominant negative (DN) AMPK, as well as AMPK shRNAs increased necroptosis and cytotoxicity induced by MNNG. We further showed that AMPK physically associated with a protein complex containing PGAM5 and Keap1 whereby facilitating Keap1-mediated PGAM5 ubiquitination upon necroptosis induction. The AMPK agonist metformin ameliorated myocardial ischemia and reperfusion (IR) injury and reduced necroptosis through down-regulating the expression of PGAM5 in the Langendorff-perfused rat hearts.

Conclusion—Activation of AMPK protects against necroptosis via promoting Keap1-mediated PGAM5 degradation. Metformin may act as a valuable agent for the protection of myocardial ischemia and reperfusion injury by activating AMPK and reducing necroptosis.

Keywords

AMP-activated protein kinase (AMPK); necroptosis; Keap1-PGAM5 complex; metformin; ischemia and reperfusion injury

1. Introduction

The AMP-activated protein kinase (AMPK) is a cell energy sensor [1,2]. Under lowered intracellular ATP levels, AMP or ADP directly binds to the γ regulatory subunit of AMPK, leading to a conformational change that promotes AMPK phosphorylation and protects AMPK from dephosphorylation to ensure its activation. Phosphorylation of Thr 172 in the activation loop of AMPKα is required for AMPK activation by LKB1, CaMKKβ, and TAK1. Activated AMPK phosphorylates and inactivates a number of metabolic enzymes involved in ATP-consuming cellular events including fatty acid, cholesterol and protein synthesis, and activates ATP-generating processes including the uptake and catabolism of glucose and fatty acids, hence maintaining the cellular energy balance. Activated AMPK may also regulate cell cycle, inhibit cell proliferation, maintain cell polarity, induce autophagy, and enhance cerebral amyloid-β clearance [1].

Phosphoglycerate mutase 5 (PGAM5) is one of the 12 members of the PGAM family. PGAM5 and two other members of the family, STS1 and STS2, are protein phosphatases although most PGAM members catalyze the phosphorylation of metabolites [3]. PGAM5 is an atypical mitochondrial Ser/Thr phosphatase that modulates mitochondrial fragmentation and cell death [3]. PGAM5 localizes to the outer membrane of mitochondria with its C terminus facing the cytoplasm. There are two splice variants of PGAM5, PGAM5L (long form) and PGAM5S (short form). Overexpression of the PGAM5S isoform results in a disconnected punctuate mitochondrial pattern, a typical phenotype of apoptosis, but without disruption of the mitochondrial membrane permeability potential and cytochrome C release [3,4]. Recent studies showed that PGAM5 is required for TNFR-triggered and reactive oxygen species (ROS)-induced intrinsic necroptosis, indicating that PGAM5 locates at the

convergence point of multiple necrotic pathways [5]. Upon activation of the extrinsic necroptosis pathway, PGAM5L tethers necrosome complex II consisting of receptor interacting protein kinase-1 (RIP1), RIP3, and mixed lineage kinase domain-like (MLKL) protein to PGAM5S on the mitochondrial membrane. Subsequently, RIP3 mediates PGAM5S phosphorylation, leading to the activation of the PGAM5S-Drp-1 axis that induces necroptosis [5,6].

Keap1 is a Bric-a-Brac (BTB)-Kelch substrate adaptor protein for a Cul3-dependent ubiquitin ligase complex that functions as a sensor for thiol-reactive chemopreventive compounds and oxidative stress [7]. PGAM5 is a substrate for the redox-regulated Keap1-dependent ubiquitin ligase complex, which licenses proteasome-dependent degradation of PGAM5 [8,9]. In the current study, we report a novel function of AMPK in the suppression of necroptosis via promoting Keap1-mediated degradation of PGAM5.

2. Methods

2.1 Antibodies and chemicals

Antibodies against ACC, pho-ACC (Ser79), AMPK, pho-AMPK (Thr172), S6 and pho-S6 (Ser240/244) were purchased from Cell Signaling (Beverly, MA). Anti-RIP1, RIP3, PGAM5 and Keap1 antibodies were from Abcam Inc. (Cambridge, MA). Anti-GFP and α-tubulin monoclonal antibodies were purchased from Santa Cruz Biotechnology (Santa Cruz, CA). Antibody against pan-phosphoserine/threonine was purchased from BD Pharmingen (San Diego, CA). Antibody against GAPDH was purchased from Fitzgerald (Acton, MA). Thiazolyl blue tetrazolium bromide (MTT), N-methyl-N′-nitro-N-nitrosoguanidine (MNNG), 2-deoxy-D-glucose (2-DG), puromycin, metformin, triphenyl tetrazolium chloride and Evans blue were purchased from Sigma-Aldrich (St. Louis, MO). zVAD-fmk was purchased from Biomol International (Plymouth Meeting, PA). A-769662 was purchased from BIOTANG (Waltham, MA).

2.2 Cell lines and transfection

Wild-type (WT) and AMPKα$^{-/-}$ mouse embryonic fibroblasts (MEFs) were obtained from Dr. Laderoute lab [10]. Cardiomyocyte cell lines H9C2 were obtained from the American Type Culture Collection. Cells were grown in Dulbecco's modified Eagle's medium (DMEM) containing 10% fetal bovine serum (FBS) in a humidified incubator containing 5% CO2 at 37 °C. pECE-AMPKα2-WT, constitutively active AMPKα2 (AMPKα2-CA) (by truncating AMPKα2 cDNA at the position corresponding to amino acid 310) and dominant negative AMPKα2-K45R (AMPKα2-DN) plasmids were provided by Dr. Anne Brunet at Stanford University [11]. AMPKα2-WT, AMPKα2-CA and AMPKα2-DN fragments were further subcloned into pEGFP-C1 vector to generate GFP-AMPKα2-WT, GFP-AMPKα2-CA, and GFP-AMPKα2-DN constructs [12]. U2OS cells were transfected with these plasmids and selected with 800 μg/ml G418 for two weeks for the establishment of stable expression cell lines.

2.3 Lentiviral packaging and shRNA knockdown of PGAM5

shRNAs targeting murine PGAM5 were purchased from Open Biosystem (Lafayette, CO). Lentiviral supernatant was prepared as described previously [12]. Wild-type and AMPKα$^{-/-}$ MEFs were infected with the shRNA-PGAM5 lentiviral supernatant and selected with 2 μg/ml puromycin for two weeks. The effect of PGMA5 knockdown was verified by immunoblotting.

2.4 Cell viability and cell death assay

Cell viability was measured by the MTT assay. Cell death was determined by trypan blue (Sigma-Aldrich, MO) exclusion assay.

2.5 Co-immunoprecipitation (co-IP)

293T cells were seeded in a 6-cm dish at 1.5×10^6 cells/dish. 24 h later, protein extracts from four dishes were pre-cleared with protein G-sepharose beads (Upstate) and used for co-IP as described previously [12]. The precipitated proteins were dissolved in 30 μl 1 x SDS loading buffer and analyzed by western blotting using the appropriate antibodies.

2.6 Immunoblotting

Cells and heart samples were collected in RIPA lysis buffer. Immunoblotting was performed as described previously [12]. A total of 30 μg proteins were used for the immunoblotting, unless otherwise indicated. GAPDH or α-tubulin was used for the loading control.

2.7 Immunofluorescence

293T cells were treated with 200 μM MNNG for 10 min before fixation with 4% paraformaldehyde. Cells were then permeabilized, blocked, and incubated with first and second antibodies. The samples were observed under a confocal microscope LSM510 (Carl Zeiss Microimaging Inc.) with appropriate binning of pixels and exposure time.

2.8 Animal experiments

The animal protocols were approved by the Committee for Experimental Animals at Jilin University. Adult, healthy male Sprague-Dawley rats, weighing 180–230g and of healthy grade were approved by the Committee for the experiments. Three to eight animals were used in each group (time point). All animals received humane care and that study protocols comply with the institution's guidelines.

Langendorff-perfused rat heart model preparation, experimental drug treatment, myocardial infarction size determination, lactate dehydrogenase (LDH) and creatine kinase-MB (CK-MB) detection, histology staining, and Evans blue staining for the degree of myocardial IR injury were performed as previously reported by us and other group [13,14] and detailed in online Supplementary Methods and Fig. S1.

2.9 Statistical analysis

The unpaired t test was used for the statistical analyses between two groups. $P < 0.05$ was considered statistically significant.

3. Results

3.1 Loss of AMPKα sensitizes cells to necroptosis induction

To determine whether AMPK is involved in necrotic cell death, WT or AMPKα$^{-/-}$ MEFs were treated with DNA alkylating agent MNNG, hydrogen peroxide (H2O2), or tumor necrosis factor α (TNFα) that were previously characterized as necroptosis inducers. As shown in Fig. 1A, cell viability was markedly decreased in AMPKα$^{-/-}$ MEFs treated with MNNG as compared with WT MEFs in a dose dependent manner. To confirm the reduction in cell viability was not due to apoptosis, we pretreated WT and AMPKα$^{-/-}$ MEFs with zVAD-fmk, a pan-apoptotic inhibitor, before addition of MNNG. The cells still underwent cell death in the presence of zVAD-fmk (Fig. 1B and C). Similarly, zVAD-insensitive cell death was markedly increased in AMPKα$^{-/-}$ MEFs than in WT MEFs treated with H2O2 (Fig. 1D). TNFα induces necrotic cell death in the face of pretreatment with cycloheximide (CHX) and z-VAD [15,16]. As shown in Fig. 1E, cell viability was significantly decreased in AMPKα$^{-/-}$ MEFs compared with that in WT MEFs treated with TNF-α in the presence of CHX and z-VAD-fmk.

Next, we questioned whether activation of AMPK might prevent cells from necroptosis. We treated WT and AMPKα$^{-/-}$ MEFs with A-769662, a small molecule compound functioning as a direct activator of AMPK, in addition to MNNG. Cell viability was increased in WT MEFs treated with MNNG in the presence of A-769662, whereas there was no difference for the viability of AMPKα$^{-/-}$ MEFs treated with MNNG regardless of the co-treatment of A-769662 (Fig. 1F). 2-DG is a glucose derivative in which the 2-hydroxyl group is replaced by hydrogen, so that it disrupts glycolysis and activates AMPK [11]. Consistently, pretreatment of 2-DG promoted cell survival under the treatment of MNNG (Fig. 1G). Thus our data suggest that AMPK activation suppresses MNNG-induced necroptosis.

To further characterize the role of AMPK in the protection of necroptosis, we established U2OS-GFP, U2OS-GFP-AMPKα2-WT, and U2OS-GFP-AMPKα2-CA cell lines. Cell viability was markedly increased and cytotoxicity was decreased in AMPKα2-WT or AMPKα2-CA cells as compared to control cells in response to MNNG (Fig. 1H, I). Similar results were obtained when these cells were exposed to H_2O_2 (Fig. 1J and K). In addition, we knocked down AMPKα using siRNAs in embryonic cardiomyocyte cell line H9C2 and exposed the cells to MNNG, TNFα, and H2O2. Consistently, depletion of AMPK sensitized H9C2 cells to the treatment of these agents and abrogated the protective effect of A-769662, the AMPK activator (Fig. 1L–N). Together, our results suggest that loss of AMPKα sensitizes cells to the induction of necroptosis, whereas activation of AMPK reduces the cell death.

3.2 AMPK is activated upon necroptosis induction and inactivation of AMPK enhances necroptosis

To determine whether AMPK signaling is activated upon necroptosis induction, WT MEFs were treated with MNNG or H_2O_2 after pretreatment of z-VAD-fmk. As shown in Fig. 2A and B, exposure to either MNNG or H2O2 led to marked increases in pAMPKα (Thr172)

and pACC (Ser79) and decreases in pS6 (Ser240/244). Similarly, activation of AMPK was observed in U2OS cells treated with MNNG or H_2O_2 (Fig. 2C–F).

To further validate the role of AMPK activation in necroptosis, we exposed the cells to AMPK inhibitor compound C (CC) and analyzed cellular response to necroptosis induction. Application of CC suppressed the activation of AMPK and modestly reduced cell viability in AMPK-intact cells (Fig. 2G). Strikingly, combination of CC and H2O2 markedly reduced cell survival in WT MEFs, whereas cell viability of AMPK−/− MEFs under the treatment of H2O2 was not altered by the addition of CC (Fig. 2G). Next, expression of a dominant negative form of AMPKα2, GFP-AMPKα2-DN, was exploited to inhibit AMPK signaling. Transduction of AMPKα2-DN reduced metformin-induced AMPK activation (Fig. 2H). Moreover, MNNG-induced reduction of cell viability was further augmented due to AMPKα2-DN transduction (Fig. 2I). Taken together, our results suggest that AMPK is activated upon necroptosis induction and inactivation of AMPK signaling reduces cell survival under the treatment of necroptosis inducers.

3.3 AMPK regulates PGAM5 expression and forms a complex with PGAM5 and Keap1

Upon necroptosis induction, RIP1 and RIP3 form a complex with MLKL and further activate the mitochondrial phosphatase PGAM5 to trigger the necroptosis process [5]. We found that AMPKα−/− MEFs possessed a high level of PGAM5 as compared with WT cells, and treatment with MNNG further increased the level of PGAM5 (Fig. 3A). In contrast, expressions of RIP3 and RIP1 were marginally decreased in AMPKα−/− MEFs (Fig. 3A). Moreover, PGAM5 expression was decreased in U2OS cells transfected with either GFP-AMPKα2-WT or GFP-AMPKα2-CA in response to H_2O_2 although the expression of RIP1 was not altered (Fig. 3B).

To further determine the impact of PGAM5 on AMPK-mediated protection of necroptosis, stable cell lines expressing shRNA-PGAM5 were established in WT and AMPKα−/− MEFs (Fig. 3C). Knockdown of PGAM5 substantially reduced cellular sensitivity to MNNG in WT and AMPK−/− MEFs (Fig. 3D). The increased cytotoxicity of AMPKα−/− MEFs versus WT MEFs upon MNNG or H_2O_2 treatment was also partially reversed following PGAM5 knockdown (Fig. 3E and F).

Next, we tested whether over-expression of PGAM5 might be sufficient to abrogate the protective effect of AMPK on necroptosis. As shown in Fig. 3G and H, over-expression of PGAM5 reduced cell viability and abolished the protective effect of 2-DG upon the application of MNNG. Further GFP-AMPKα2-CA did not exhibit any protective effects against MNNG or H2O2 treatment when PGAM5 was over-expressed (Fig. 3I and J).

PGAM5 is a substrate for the redox-regulated Keap1-dependent ubiquitin ligase complex [8,9]. To determine whether AMPK regulates PGAM5 through Keap1, we exposed the U2OS control, U2OS/GFP-AMPKα2-WT, and U2OS/GFP-AMPKα2-CA cells to MNNG or H2O2 and detected the expression of Keap1. Relatively higher levels of Keap1 were detected in WT- and AMPKα2-CA cells as compared with the parental cells, and Keap1 levels in the cells were further increased following exposure to H_2O_2 or MNNG (Fig. 3K and L).

To explore the potential mechanisms whereby AMPK regulates Keap1-PGAM5, we transfected 293T cells with PGAM5 and GFP-AMPKα2-CA and performed co-IP assays. Both GFP-AMPKα2-CA (Fig. 3M) and PGAM5 (Fig. 3N) were present in each other's immunoprecipitates, suggesting that PGAM5 is associated with AMPKα2. Further, we found that Keap1 was also included in the AMPK-PGAM5 complex when PGAM5, Keap1, and GFP-AMPKα2-CA were co-expressed and analyzed with reciprocal co-IPs (Fig. 3O–Q). Thus, we conclude that AMPK, Keap1, and PGAM5 are physically associated.

To further verify the interactions among AMPK, PAGM5 and Keap1, immunofluorescence staining was performed in 293T cells treated with MNNG. As shown in Fig. 3R and S, Keap1 was co-localized with AMPKα as well as PGAM5, and the co-localization was strongly induced upon MNNG (Data not shown). Taken together, these data indicate that AMPK is associated with the PGAM5-Keap1 complex.

3.4 AMPK promotes Keap1-mediated ubiquitination of PGAM5

Keap1 has been reported to mediate the ubiquitination of PGAM5 [3,9]. We then sought to interrogate whether AMPK down-regulates PGAM5 through Keap1-mediated ubiquitination. To assay the rate of Keap1 protein turnover, WT and AMPKα$^{-/-}$ MEFs were treated with CHX to inhibit protein synthesis. The levels of Keap1 were determined at different time points after the addition of CHX. The half-life of Keap1 protein was more than 4 h in WT MEFs, but it was shortened to 2 h in AMPK-deficient MEFs (Fig. S2A and B), indicating that Keap1 becomes unstable in the absence of AMPK.

To determine whether the ubiquitination of PGAM5 is regulated by AMPK, we co-transfected 293T cells with HA-ubiquitin, PGAM5, Keap1, and/or GFP-AMPKα2-CA constructs (Fig. S2C). The presence of HA-ubiquitin conjugation onto PGAM5 protein was measured by anti-HA immunoblot analysis of anti-PGAM5 immunoprecipitates. As shown in Fig. S2D, a marked increase in ubiquitin conjugation onto PGAM5 was observed in the presence of co-expressed GFP-AMPKα2-CA, revealing a role of AMPK in the promotion of PGAM5 ubiquitination.

3.5 AMPK attenuates ischemia/reperfusion (IR)-induced myocardial necroptosis and improves cardiac function in Langendorff heart

To identify whether activation of AMPK reduces necroptosis in vivo, we treated the Langendorff-perfused rat hearts with metformin, an antidiabetic agent that activates AMPK, and monitored the IR injury. It showed that application of metformin substantially attenuated post-ischemic myocardial infarction (Fig. 4A and B), with reduced LDH and CK-MB levels (Fig. 4C and D) and histopathological necrotic areas (Fig. 4E) and improved cardiac function (Fig. 4F). Evans blue dye uptake, an indicator for measuring the necroptosis after IR injury, was markedly decreased in rat hearts treated with metformin (Fig. 4G and H). Furthermore, metformin did not exhibit any cardioprotective effects against IR injury when activation of AMPK was suppressed with the treatment of compound C (Fig. 4A–H). Consistent with the notion that activation of AMPK protects cardiomyocytes from necroptosis in vivo, the levels of pAMPK and Keap1 were increased, whereas PGAM5 was decreased in metformin-treated hearts. Co-administration of compound C with metformin

largely abolished the effects of metformin on these biochemical markers (Fig. 4I). Taken together, our results suggest that activation of AMPK by metformin lessens IR-injury-induced necroptosis (Fig. 4J).

4. Discussion

In the current study, we reported that AMPK protected MEFs and cardiomyocytes from MNNG- and ROS-induced necroptosis. AMPK activators A-769662 and 2-DG reduced cell necroptosis after MNNG treatment in these cells (Fig. 1). In contrast, inactivation of AMPK enhanced necroptosis induction (Fig. 2). More importantly, our in vivo study demonstrated that application of AMPK activator metformin attenuated IR-induced myocardial necroptosis and improved cardiac function in Langendorff heart model.

Wang et al. [5] reported that PGAM5 is phosphorylated by RIP3 under necroptosis induction, leading to an increased PGAM5 phosphatase activity. Strikingly, dynamin-related protein 1 (DRP1), a GTPase that controls mitochondrial fission was found to be recruited to the necrosome by PGAM5S, the short form of PGAM5, and to be subsequently activated through the PGAM5S phosphatase activity. Knockdown of PGAM5S or DRP1 prevented necroptosis, indicating that recruitment and activation of DRP1 by PGAM5S are crucial for the execution of this pathway [5]. Although the role of PGAM5 activation in necroptosis prompted by different inducers may not be generalizable [17–20], investigators indeed provided unarguable evidence demonstrating that PGAM5 is located at the convergence point of the necrotic pathways in TNFα, ROS, and calcium ionophore-induced necroptosis. In the current study, we demonstrated that AMPK-induced protection against necroptosis was mediated via downregulation of PGAM5, supporting the critical role of PGAM5 in necroptosis.

PGAM5 is a substrate for the redox-regulated Keap1-dependent ubiquitin ligase complex [3]. Ablation of Keap1 signaling reduces macrophage/neutrophil trafficking, pro-inflammatory cytokine programs, and hepatocellular necroptosis/apoptosis [21]. Moreover, activation of Keap1 increases the level of intracellular ROS, which further leads to a thioredoxin-dependent increase in a reduced state of Keap1, hence promoting PGAM5 and Bcl-xL degradation in prostate cancer cells [22]. We cotransfected PGAM5, Keap1 and GFP-AMPKα2-CA constructs into 293T cells and demonstrated that AMPK was associated with Keap1 and PGAM5 complex (Fig. S2). Further, we confirmed that activation of AMPK increased the ubiquitination of PGAM5, which most probably resulted from the stabilization of Keap1 (Fig. S2).

Accumulating evidence suggests that mitochondrial fission characterized by fragmentation and the disappearance of cristae membranes and the formation of small, round, disconnected units of mitochondria occurs early in necrotic cell death and is a causal event for necroptosis [23,24]. Consistently, PGAM5 was found to regulate mitochondrial fission in a context-dependent manner [5]. In a recent report, interestingly, Toyama et al. [2] found that AMPK is activated and phosphorylates DRP1 receptor protein MFF (mitochondrial fission factor) under stresses and hence promotes the relocation of DRP1 to the outer membrane of mitochondria and the formation of mitochondrial fission. The increased fission induced by

AMPK facilitates selective elimination of the damaged mitochondria through mitophagy, which may act as a quality-control response to stresses.

Although starvation or deprivation of glucose also leads to the increase of AMP and the decrease of ATP and hence activates AMPK, neither of them physiologically results in fission, but contrarily suppresses the process, inducing mitochondria to elongate [25,26]. It remains unknown how different stresses that activate AMPK lead to distinct mitochondrial responses. Modulation of DRP1 expression, location, and phosphorylation may contribute to various responses. There is evidence showing that starvation of cells and/or activation of AMPK induce DRP1 phosphorylation at S637, which has been linked to the inhibition of DRP1 and a decrease in mitochondrial fission [25–28]. In addition, recent studies revealed that pharmacological activation of AMPK by 2-DG, AICAR, and metformin downregulates the expression of DRP1 and reduces its translocation into mitochondria in endothelial cells, cardiomyocytes, and hepatocytes, hence prevents mitochondrial fragmentation and dysfunction [29–32]. Moreover, it was found that PRKAA (AMPKα gene) deletion inhibits autophagy-dependent degradation of DNM1L (dynamin 1-like), a mitochondrial fission protein that promotes mitochondrial fragmentation in vascular endothelial cells [33]. In the current study, we characterized a new mechanism by which AMPK acts in necroptosis regulation and possibly in mitochondrial integrity through enhancing the degradation of PGAM5 (Fig. 4J). Collectively, these data suggest that activation of AMPK plays a role in mitochondrial homeostasis at multiple layers, highlighting the importance of fine-tuning mitochondrial fission/fusion responses to different stimuli. AMPK works in the context of other cellular signals to promote a variety of mitochondrial functions, including the execution of necroptosis.

Necroptosis is of central pathophysiological process relevant to the development of multiple diseases, such as ischemia-reperfusion injury, myocardial infarction, atherosclerosis, stroke, pancreatitis, and inflammatory bowel disease [34–36]. Administration of necroptosis inhibitor necrostatin-1 substantially reduced infarct size [34,37], inhibited RIP1/RIP3 phosphorylation, and significantly suppressed cell death in guinea pig and mouse I/R heart models, confirming the involvement of the necroptotic pathway in cardiomyocyte injury. Metformin is an efficient activator of AMPK and used in clinic for the treatment of diabetes for decades with no significant side effects. Thus, we questioned whether metformin is able to ameliorate I/R injury, in particular necroptosis, by activation of AMPK. We found that AMPK activation by metformin inhibited the expression of PGAM5, reduced necroptosis, and exerted a markedly cardioprotective effect. The anti-necrotic effect of metformin was abrogated in rat hearts after AMPK suppression (Fig. 4A–I). Taken together, our study provides in vivo evidence demonstrating that AMPK plays an important role in the protection of necroptosis and activation of AMPK with activators, such as metformin, could be a valuable method for the improvement of myocardial I/R injury.

4.1. Limitations

In the study, we used MNNG, H2O2, and TNFα to induce necroptosis. MNNG is a DNA-alkylating agent, administration of which could activate PARP-1 and stimulate the synthesis of PAR, leading to parthanatos, another form of regulated necrosis [38]. Although some

investigators consider parthanatos and necroptosis as two subsets of programmed necrosis sharing similar phenotypes [39], these two types of necrosis possess individual molecular characteristics [40]. We did not specify the contribution of parthanatos to necroptosis we analyzed and could not rule out the potential existence of parthanatos in MNNG-induced necrosis.

5. Conclusions

AMPK is activated upon necroptosis induction. Activated AMPK protects cells from necroptosis by promoting Keap1-mediated PGAM5 degradation. The AMPK agonist metformin reduces cadiomyocyte necroptosis and ameliorates myocardial IRI. Metformin may act as a valuable agent for the protection of myocardial damage.

Supplementary Material

Refer to Web version on PubMed Central for supplementary material.

Acknowledgments

We thank Dr. Mark Hannink at the University of Missouri for providing the PGAM5 plasmids (FLAG-PGAM5-L, FLAG-PGAM5-S, and FLAG-PGAM5-L-E79A/S80A), Dr. Anne Brunet at Stanford University for providing the pECE-AMPKα2-WT, AMPKα2-CA, and AMPKα2-DN plasmids, and Dr. Keith Laderoute at SRI International for providing WT and AMPKα−/− MEFs.

References

1. Hardie DG, Schaffer BE, Brunet A. AMPK: An Energy-Sensing Pathway with Multiple Inputs and Outputs. Trends Cell Biol. 2016; 26:190–201. [PubMed: 26616193]
2. Toyama EQ, Herzig S, Courchet J, et al. AMP-activated protein kinase mediates mitochondrial fission in response to energy stress. Science. 2016; 351:275–281. [PubMed: 26816379]
3. Wilkins JM, McConnell C, Tipton PA, Hannink M. A conserved motif mediates both multimer formation and allosteric activation of phosphoglycerate mutase 5. J Biol Chem. 2014; 289:25137–25148. [PubMed: 25012655]
4. Hammond PW, Alpin J, Rise CE, Wright M, Kreider BL. In vitro selection and characterization of Bcl-X(L)-binding proteins from a mix of tissue-specific mRNA display libraries. J Biol Chem. 2001; 276:20898–20906. [PubMed: 11283018]
5. Wang Z, Jiang H, Chen S, Du F, Wang X. The mitochondrial phosphatase PGAM5 functions at the convergence point of multiple necrotic death pathways. Cell. 2012; 148:228–243. [PubMed: 22265414]
6. Sun L, Wang H, Wang Z, et al. Mixed lineage kinase domain-like protein mediates necrosis signaling downstream of RIP3 kinase. Cell. 2012; 148:213–227. [PubMed: 22265413]
7. Canning P, Bullock AN. New strategies to inhibit KEAP1 and the Cul3-based E3 ubiquitin ligases. Biochem Soc Trans. 2014; 42:103–107. [PubMed: 24450635]
8. Lo SC, Hannink M. PGAM5, a Bcl-XL-interacting protein, is a novel substrate for the redox-regulated Keap1-dependent ubiquitin ligase complex. J Biol Chem. 2006; 281:37893–37903. [PubMed: 17046835]
9. Suzuki T, Maher J, Yamamoto M. Select heterozygous Keap1 mutations have a dominant-negative effect on wild-type Keap1 in vivo. Cancer Res. 2011; 71:1700–1709. [PubMed: 21177379]
10. Laderoute KR, Amin K, Calaoagan JM, et al. 5′-AMP-activated protein kinase (AMPK) is induced by low-oxygen and glucose deprivation conditions found in solid-tumor microenvironments. Mol Cell Biol. 2006; 26:5336–5347. [PubMed: 16809770]

11. Greer EL, Oskoui PR, Banko MR, et al. The energy sensor AMP-activated protein kinase directly regulates the mammalian FOXO3 transcription factor. J Biol Chem. 2007; 282:30107–30119. [PubMed: 17711846]
12. Liang J, Xu ZX, Ding Z, et al. Myristoylation confers noncanonical AMPK functions in autophagy selectivity and mitochondrial surveillance. Nat Commun. 2015; 6:7926. [PubMed: 26272043]
13. Zhang J, Wang C, Yu S, et al. Sevoflurane postconditioning protects rat hearts against ischemia-reperfusion injury via the activation of PI3K/AKT/mTOR signaling. Sci Rep. 2014; 4:7317. [PubMed: 25471136]
14. Pasdois P, Parker JE, Griffiths EJ, Halestrap AP. Hexokinase II and reperfusion injury: TAT-HK2 peptide impairs vascular function in Langendorff-perfused rat hearts. Circ Res. 2013; 112:e3–7. [PubMed: 23329796]
15. Burchfield JS, Dong JW, Sakata Y, et al. The cytoprotective effects of tumor necrosis factor are conveyed through tumor necrosis factor receptor-associated factor 2 in the heart. Circ Heart Fail. 2010; 3:157–164. [PubMed: 19880804]
16. Babu D, Leclercq G, Goossens V, et al. Antioxidant potential of CORM-A1 and resveratrol during TNF-α/cycloheximide-induced oxidative stress and apoptosis in murine intestinal epithelial MODE-K cells. Toxicol Appl Pharmacol. 2015; 288:161–178. [PubMed: 26187750]
17. Moriwaki K, Farias Luz N, Balaji S, et al. The Mitochondrial Phosphatase PGAM5 Is Dispensable for Necroptosis but Promotes Inflammasome Activation in Macrophages. J Immunol. 2016; 196:407–415. [PubMed: 26582950]
18. He GW, Günther C, Kremer AE, et al. PGAM5-mediated programmed necrosis of hepatocytes drives acute liver injury. Gut. 2017; 66:716–723. [PubMed: 27566130]
19. Lu W, Sun J, Yoon JS, et al. Mitochondrial Protein PGAM5 Regulates Mitophagic Protection against Cell Necroptosis. PLoS One. 2016; 11:e0147792. [PubMed: 26807733]
20. Kang YJ, Bang BR, Han KH, et al. Regulation of NKT cell-mediated immune responses to tumours and liver inflammation by mitochondrial PGAM5-Drp1 signalling. Nat Commun. 2015; 6:8371. [PubMed: 26381214]
21. Ke B, Shen XD, Zhang Y, et al. KEAP1-NRF2 complex in ischemia-induced hepatocellular damage of mouse liver transplants. J Hepatol. 2013; 59:1200–1207. [PubMed: 23867319]
22. Xu Y, Fang F, Miriyala S, et al. KEAP1 is a redox sensitive target that arbitrates the opposing radiosensitive effects of parthenolide in normal and cancer cells. Cancer Res. 2013; 73:4406–4417. [PubMed: 23674500]
23. Youle RJ, van der Bliek AM. Mitochondrial Fission, Fusion, and Stress. Science. 2012; 337:1062–1065. [PubMed: 22936770]
24. Chan FK, Baehrecke EH. RIP3 finds partners in crime. Cell. 2012; 148:17–18. [PubMed: 22265396]
25. Rambold AS, Kostelecky B, Elia N, Lippincott-Schwartz J. Tubular network formation protects mitochondria from autophagosomal degradation during nutrient starvation. Proc Natl Acad Sci U S A. 2011; 108:10190–10195. [PubMed: 21646527]
26. Gomes LC, Di Benedetto G, Scorrano L. During autophagy mitochondria elongate, are spared from degradation and sustain cell viability. Nat Cell Biol. 2011; 13:589–598. [PubMed: 21478857]
27. Wikstrom JD, Israeli T, Bachar-Wikstrom E, et al. AMPK regulates ER morphology and function in stressed pancreatic β-cells via phosphorylation of DRP1. Mol Endocrinol. 2013; 27:1706–1723. [PubMed: 23979843]
28. Chang CR, Blackstone C. Cyclic AMP-dependent protein kinase phosphorylation of Drp1 regulates its GTPase activity and mitochondrial morphology. J Biol Chem. 2007; 282:21583–21587. [PubMed: 17553808]
29. Wang Q, Zhang M, Torres G, et al. Metformin Suppresses Diabetes-Accelerated Atherosclerosis via the Inhibition of Drp1-Mediated Mitochondrial Fission. Diabetes. 2017; 66:193–205. [PubMed: 27737949]
30. Sakamoto A, Saotome M, Hasan P, et al. Eicosapentaenoic acid ameliorates palmitate-induced lipotoxicity via the AMP kinase/dynamin-related protein-1 signaling pathway in differentiated H9c2 myocytes. Exp Cell Res. 2017; 351:109–120. [PubMed: 28088331]

31. Zhang C, Huang J, An W. Hepatic stimulator substance resists hepatic ischemia/reperfusion injury by regulating Drp1 translocation and activation. Hepatology. 2017 Jun 23. Epub ahead of print. doi: 10.1002/hep.29326
32. Yang X, Wang H, Ni HM, et al. Inhibition of Drp1 protects against senecionine-induced mitochondria-mediated apoptosis in primary hepatocytes and in mice. Redox Biol. 2017; 12:264–273. [PubMed: 28282614]
33. Wang Q, Wu S, Zhu H, et al. Deletion of PRKAA triggers mitochondrial fission by inhibiting the autophagy-dependent degradation of DNM1L. Autophagy. 2017; 13:404–422. [PubMed: 28085543]
34. Linkermann A, Green DR. Necroptosis. N Engl J Med. 2014; 370:455–465. [PubMed: 24476434]
35. Linkermann A, Bräsen JH, Himmerkus N, et al. Rip1 (receptor-interacting protein kinase 1) mediates necroptosis and contributes to renal ischemia/reperfusion injury. Kidney Int. 2012; 81:751–761. [PubMed: 22237751]
36. Oerlemans MI, Liu J, Arslan F, et al. Inhibition of RIP1-dependent necrosis prevents adverse cardiac remodeling after myocardial ischemia-reperfusion in vivo. Basic Res Cardiol. 2012; 107:270–276. [PubMed: 22553001]
37. Koshinuma S, Miyamae M, Kaneda K, Kotani J, Figueredo VM. Combination of necroptosis and apoptosis inhibition enhances cardioprotection against myocardial ischemia-reperfusion injury. J Anesth. 2014; 28:235–241. [PubMed: 24113863]
38. Andrabi SA, Umanah GK, Chang C, et al. Poly(ADP-ribose) polymerase-dependent energy depletion occurs through inhibition of glycolysis. Proc Natl Acad Sci U S A. 2014; 111:10209–10214. [PubMed: 24987120]
39. Nagley P, Higgins GC, Atkin JD, Beart PM. Multifaceted deaths orchestrated by mitochondria in neurones. Biochim Biophys Acta. 2010; 1802:167–185. [PubMed: 19751830]
40. Fatokun AA, Dawson VL, Dawson TM. Parthanatos: mitochondrial-linked mechanisms and therapeutic opportunities. Br J Pharmacol. 2014; 171:2000–2016. [PubMed: 24684389]

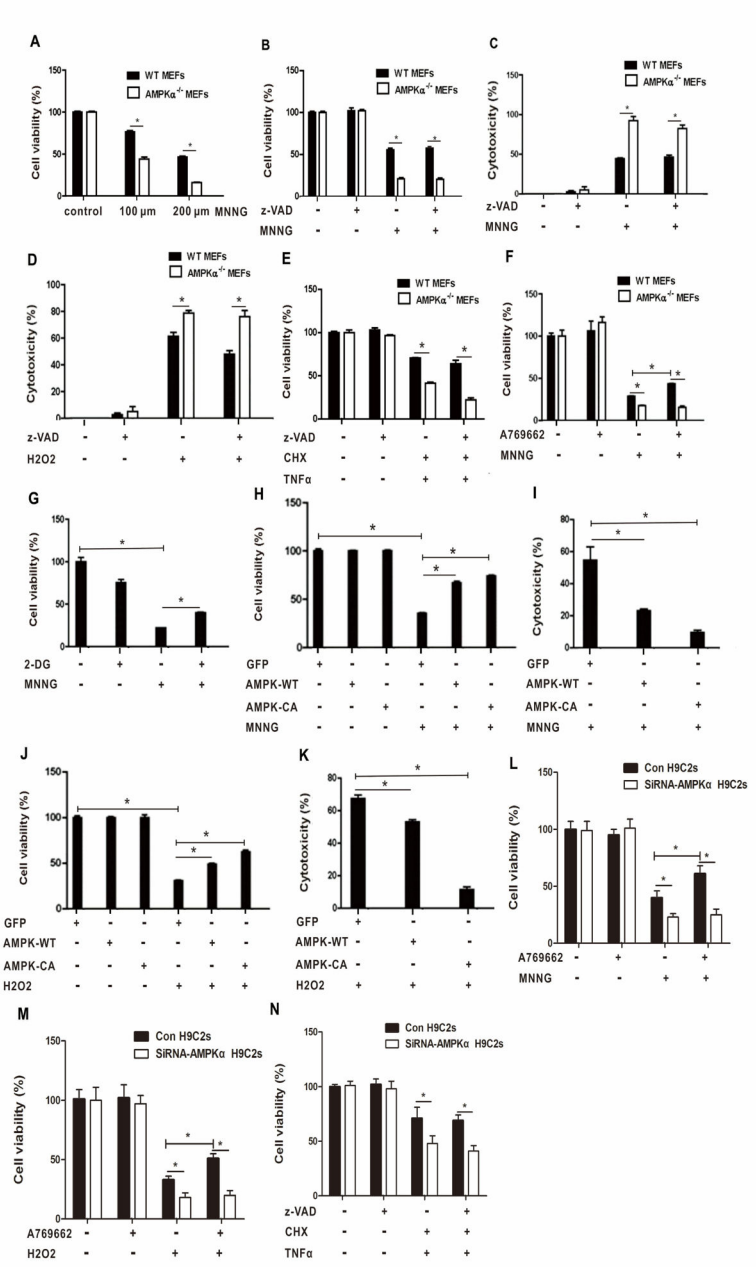

Fig. 1.

Loss of AMPKα sensitizes cells to necroptosis induction. (A) WT and AMPKα-null MEFs were treated with 100 μM or 200 μM MNNG for 10 min. The cells were cultured in fresh medium for 24 h. Cell viability was measured by MTT assay. (B) WT and AMPKα-null MEFs were pretreated with z-VAD (50 μM) for 2 h, followed by treatment with 200 μM MNNG for 10 min. The cells were cultured in fresh medium for 24 h. Cell viability was measured by MTT assay. (C) WT and AMPKα-null MEFs were treated as described in (A). The supernatant was collected. Cytotoxicity was determined by LDH assay. (D) WT or AMPKα-null MEFs were treated with 50 μM H_2O_2 for 24 h. Cytotoxicity was determined by LDH assay. (E) WT or AMPKα-null MEFs were pretreated with CHX (10 μg/ml) and z-

VAD (50 μM) for 2 h, followed by treatment with TNFα (150 ng/ml) for 24 h. Cell viability was measured by MTT assay. (F) WT or AMPKα-null MEFs were pretreated with A769662 (20 μM) for 2 h, followed by treatment of 200 μM MNNG for 10 min. The cells were then cultured in fresh medium for 24 h. Cell viability was measured by MTT assay. (G) U2OS cells were pretreated with 2-DG (10 mM) for 1 h, followed by treatment of MNNG (100 μM) for 15 min. The cells were then cultured in fresh medium for 24 h. Cell viability was measured by MTT assay. (H, I,). U2OS-GFP, U2OS-GFP-AMPKα2-WT and U2OS-GFP-AMPKα2-CA cells were treated with 100 μM MNNG for 15 min, and then cultured in fresh medium. Twenty four hours later, cell viability (H) and cytotoxicity (I) were determined by MTT and LDH assay, respectively. (J, K) U2OS-GFP, U2OS-GFP-AMPKα2-WT and U2OS-GFP-AMPKα2-CA cells were treated with H_2O_2 (600 μM) for 1 h. Cell viability (J) and cytotoxicity (K) were measured by MTT and LDH assay, respectively. (L, M) H9C2 cells were pretreated with A769662 (20 μM) for 2 h, followed by treatment of 100 μM MNNG for 15 min (L) or 600 μM H_2O_2 for 1 h (M). Cell viability was measured by MTT assay after 24 h. (N) H9C2 cells were pretreated with CHX (10 μg/ml) and z-VAD (50 μM) for 2 h, followed by treatment with TNFα (150 ng/ml) for 24 h. Cell viability was measured by MTT assay. All data are presented as mean ± SEM of triplicates. * $P < 0.05$.

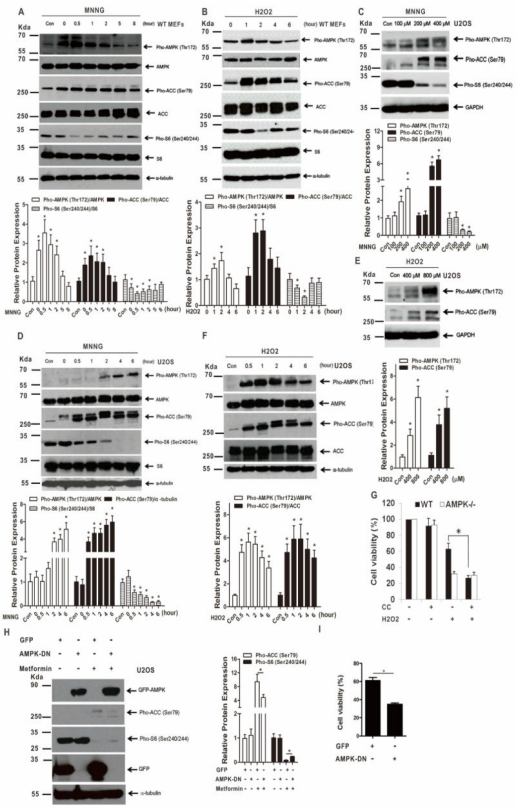

Fig. 2.

AMPK is activated upon necroptosis induction and inactivation of AMPK enhances necroptosis. (A) MEFs were treated with 200 μM MNNG for 10 min and cultured with fresh medium. The cells were collected at the indicated time points after the treatment. Cell lysates were subjected to western blot analysis. (B) MEFs were treated with 50 μM H2O2 for the indicated time points. Cell lysates were subjected to western blot analysis. (C) U2OS cells were treated with MNNG at the indicated concentrations for 15 min and cultured with fresh medium. Cell lysates were subjected to western blot 2 h after the treatment. (D) U2OS cells were treated with 200 μM MNNG for the indicated time points. Cell lysates were subjected to western blot analysis. (E) U2OS cells were treated with H2O2 at the indicated concentrations for 2 h. Cell lysates were subjected to western blot analysis. (F) U2OS cells were treated with 600 μM H2O2. Cell lysates were collected at the indicated time points and subjected to western blot analysis. (G) WT and AMPK−/− MEFs were pretreated with compound C (10 μM) for 1 h, followed by treatment of H_2O_2 (600 μM) for 2 h. Cell viability was measured by MTT assay after 24 h. (H) U2OS-GFP and U2OS-GFP-AMPKα2-DN cells were treated with metformin (10 mM) for 24 h. Cell lysates were subjected to western blot. (I) U2OS-GFP and U2OS-GFP-AMPKα2-DN cells were treated with MNNG (100 μM) for 15 min. The cells were washed and cultured in fresh medium for 24 h. Cell viability was determined by MTT assay. The values were normalized with samples treated with DMSO. Relative protein expression in each western blot was determined with ImageJ. All data are presented as mean ± SEM of triplicates. * $P < 0.05$.

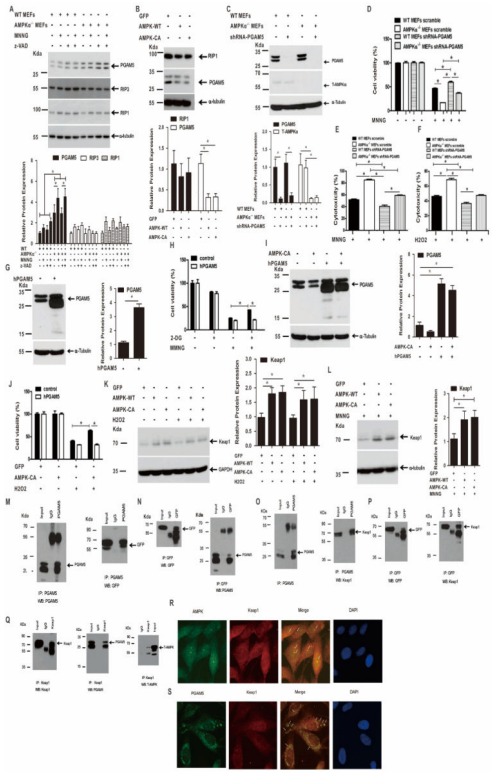

Fig. 3.

AMPK regulates PGAM5 expression and forms a complex with PGAM5 and Keap1. (A) WT and AMPKα-null MEFs were pretreated with z-VAD (50 μM) for 2 h, followed by treatment with 200 μM MNNG for 10 min. The cells were washed and cultured in fresh medium for 2 h before harvest. Cell lysates were subjected to western blot analysis. (B) U2OS-GFP, U2OS-GFP-AMPKα2-WT and U2OS-GFP-AMPKα2-CA cells were treated with H_2O_2 (600 μM) for 1 h. Cell lysates were collected and subjected to western blot analysis. (C) WT and AMPKα-null MEFs were infected with lentiviruses expressing shRNA-PGAM5 or scramble shRNA and selected with 2 μg/ml puromycin for two weeks to establish stable cell lines. Expression of PGAM5 in the cells was analyzed with western blot. (D, E) The indicated cell lines were treated with MNNG (200 μM) for 10 min and then cultured in fresh medium for 24 h. Cell viability (D) and cytotoxicity (E) were determined by MTT and LDH assay, respectively. (F) The indicated cell lines were treated with H_2O_2 (50 μM) for 24 h. Cytotoxicity was determined by LDH assay. (G) U2OS cells were transfected with pCMV-SPORT6control or pCMV-SPORT6/human PGAM5S plasmid for 48 h. Cell lysates were subjected to western blot analysis. (H) The transfected cells were pretreated with 2-DG (10 mM) for 1 h, and then treated with MNNG (100 μM, 15 min). Cell viability was measured by MTT assay. (I, J) U2OS-GFP and U2OS-GFP-AMPKα2-CA cells were transfected with pCMV-SPORT6 empty vector or pCMV-SPORT6/human PGAM5S plasmid for 48 h. Cell lysates were subjected to western blot (I). The transfected cells were treated with H_2O_2 (50 μM) for 24 h. Cell viability was measured by MTT assay (J). All data are presented as mean ± SEM of triplicates. * $P < 0.05$. (K) U2OS-GFP, U2OS-GFP-AMPKα2-WT and U2OS-GFP-AMPKα2-CA cells were treated with or without H_2O_2

(600 μM) for 1 h. Cell lysates were subjected to western blot analysis. (L) 293T cells were transiently transfected with pEGFP-c1 or pEGFP-AMPK-WT or pEGFP-AMPK-CA plasmids. Forty eight hours later, cells were treated with MNNG (100 μM) for 15 min and maintained in fresh medium. Cells lysates were collected and subjected to western blot 1 h after the treatment of MNNG. (M, N) 293T cells were transfected with human PGAM5 and U2OS-GFP-AMPKα2-CA plasmids for 48 h. Cell lysates were collected and incubated with rabbit IgG control or PGAM5 Ab, followed by immunoprecipitation with protein A/G magnetic beads (M). The immunoprecipitate was analyzed by western blot with PGAM5 Ab or GFP Ab, respectively. In a reciprocal experiment, cell lysates were incubated with mouse IgG control or GFP Ab, followed by immunoprecipitation with protein A/G magnetic beads (N). The immunoprecipitate was determined with western blot with GFP or PGAM5, respectively. (O, P) 293T cells were transfected with human PGAM5, GFP-AMPKα2-CA and Keap1 plasmids for 48 h. Cell lysates were incubated with rabbit IgG control or PGAM5 Ab, followed by immunoprecipitation with protein A/G magnetic beads (O). The immunoprecipitate was examined by immunoblotting with PGAM5 Ab or Keap1 Ab, respectively. In parallel, cell lysates were incubated with mouse IgG control or GFP Ab, followed by immunoprecipitation with protein A/G magnetic beads (P). The immunoprecipitate was also determined by immunoblotting with GFP or Keap 1 Ab, respectively. (Q) 293T cells were transfected with human PGAM5, GFP-AMPKα2-CA and Keap1 plasmids for 48 h. Cell lysates were incubated with mouse IgG control or Keap1 Ab, followed by immunoprecipitation with protein A/G magnetic beads. The immunoprecipitate was examined by immunoblotting with Keap1 Ab or PGAM5 Ab or AMPK Ab, respectively. (R, S) Confocal fluorescence microscopy probing for AMPK (green) and Keap1 (red) (R) or PGAM5 (green) and Keap1 (red) (S) in 293T cells treated with MNNG. White arrows denote co-localizing proteins. Representative images are obtained from two independent experiments.

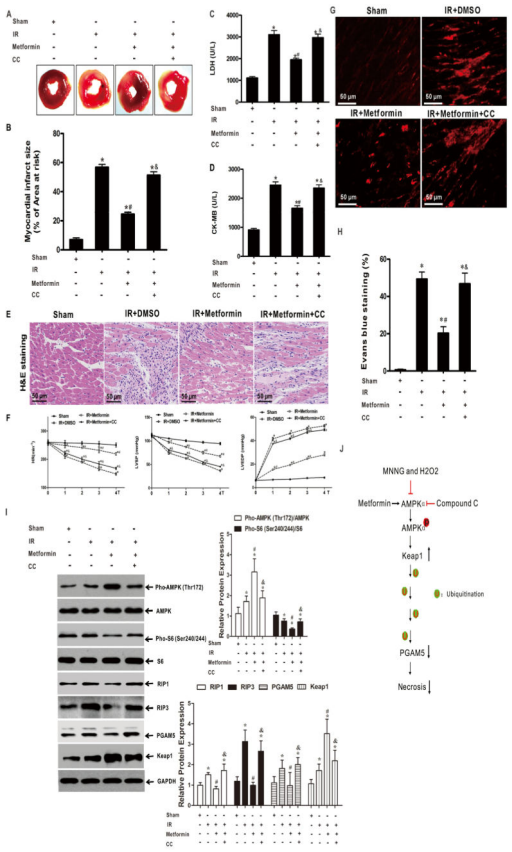

Fig. 4.

Activation of AMPK with metformin attenuates ischemia/reperfusion (IR)-induced myocardial necroptosis. Sprague Dawley rats were treated as described in Supplementary Methods for the establishment of IR-induced myocardial necroptosis model. (A) At the end of reperfusion, myocardial infraction size was determined by 1% TTC staining. (B) Quantification of infarct sizes in the TTC staining (n = 6/group). (C, D) LDH and CK-MB levels were detected by ELISA. (E) Myocardial pathological changes were measured by HE staining (scar bar = 50 μm, n = 3/group). (F) The hemodynamic parameters were recorded continuously in the period of ischemia reperfusion (n = 6–8/group). (G, H) Analysis of IR injury induced necroptosis via Evans blue dye uptake in the hearts. The percent area of EBD positive myocardium is shown (n = 4/group). (I) The isolated rat hearts were collected at the end of reperfusion and subjected to western blot analysis (n = 4/group). Relative protein expression was determined with ImageJ. (J) Schematic representation of the mechanism for AMPK-mediated protection against necroptosis via regulation of Keap1-PGAM5 complex. All data are presented as mean ± SEM of triplicates. * $P < 0.05$ vs Sham group; # $P < 0.05$ vs IR + DMSO group; & $P < 0.05$ vs IR + metformin group.